Naval Research Laboratory

Washington, DC 20375-5320

NRL/MR/5650--14-9550

Applications of Graphene to Photonics

Marc Currie

Photonics Technology Branch
Optical Sciences Division

July 1, 2014

REPORT DOCUMENTATION PAGE

Form Approved
OMB No. 0704-0188

1. REPORT DATE *(DD-MM-YYYY)*	**2. REPORT TYPE**	**3. DATES COVERED** *(From - To)*
01-07-2014	Memorandum	03-02-2014 – 24-04-2014

4. TITLE AND SUBTITLE

Applications of Graphene to Photonics

5a. CONTRACT NUMBER

5b. GRANT NUMBER

5c. PROGRAM ELEMENT NUMBER

6. AUTHOR(S)

Marc Currie

5d. PROJECT NUMBER
ONR 61135N

5e. TASK NUMBER
EL011-07-43

5f. WORK UNIT NUMBER
WU 4891

7. PERFORMING ORGANIZATION NAME(S) AND ADDRESS(ES)

Naval Research Laboratory, Code 5650
4555 Overlook Avenue, SW
Washington, DC 20375-5320

8. PERFORMING ORGANIZATION REPORT NUMBER

NRL/MR/5650--14-9550

9. SPONSORING / MONITORING AGENCY NAME(S) AND ADDRESS(ES)

Office of Naval Research
One Liberty Center
875 North Randolph Street, Suite 1425
Arlington, VA 22203-1995

10. SPONSOR / MONITOR'S ACRONYM(S)

ONR

11. SPONSOR / MONITOR'S REPORT NUMBER(S)

12. DISTRIBUTION / AVAILABILITY STATEMENT

Approved for public release; distribution is unlimited.

13. SUPPLEMENTARY NOTES

14. ABSTRACT

Graphene is a potential candidate for integrated carbon-based photonics. Its unique combination of mechanical, electrical, and optical properties gives it several advantages in photonic applications. Graphene's physical properties encompass large-area epitaxial monolayer growth, low-dimensional relativistic "massless" carriers, and universal optical conductivity from the visible to the infrared, to name a few. The object of this report is to provide a basic understanding of graphene and its use in photonic devices, covering the areas of photodetection, optical modulation, optical polarization, plasmonics, and nonlinear optical properties and devices.

15. SUBJECT TERMS

Graphene Optic Two-dimensional material
Photonic Electronic

16. SECURITY CLASSIFICATION OF:			**17. LIMITATION OF ABSTRACT**	**18. NUMBER OF PAGES**	**19a. NAME OF RESPONSIBLE PERSON**
a. REPORT	**b. ABSTRACT**	**c. THIS PAGE**			Marc Currie
Unclassified Unlimited	Unclassified Unlimited	Unclassified Unlimited	Unclassified Unlimited	26	**19b. TELEPHONE NUMBER** *(include area code)* (202) 404-4201

Standard Form 298 (Rev. 8-98)
Prescribed by ANSI Std. Z39.18

Contents

1 Introduction

Graphene is a two-dimensional form of carbon. It forms a hexagonal lattice with hybrid sp^2 bonding. Another way to envision graphene is as an unrolled carbon nanotube. The well known three-dimensional material graphite is formed by sheets of graphene combined in disarray.

Theory for this 2-D carbon structure is not new. A single hexagonal layer of graphite was investigated in 1947 [1] to help explain the properties of graphite. However, demonstration of the physical properties from the first isolated graphene monolayer was in 2004 by Geim and Novoselov [2], which subsequently earned them the Nobel Prize in Physics in 2010. To achieve this isolation, Geim and Novolselov applied adhesive tape to graphite (highly-oriented pyrolytic graphite, HOPG) to mechanically exfoliate the material. This essentially amounted to breaking weak van der Waals bonds holding the graphene sheets together. After performing this exfoliation many times, they produced a roughly 10 μm^2 graphene monolayer (in addition, they produced many larger multilayer graphene structures) [2]. This experiment was a catalyst for the current popular exploration of two-dimensional materials.

Graphene is a potential candidate for integrated carbon-based photonics. Its epitaxial growth makes it amenable to large-area, industrial processing. In addition, its low-dimensionality and semi-metallic nature provide a linear relationship of its electrons' momentum and energy ($k \propto \omega$). This produces relativistic "massless" carriers and a zero-gap Dirac point at the K and K' locations of the Brillouin zone. This electronic band structure provides many unique characteristics for electronics and photonics, some of which are explored here, and those not discussed demonstrate the untapped potential of graphene (and related low-dimensionality materials).

While this report attempts to review some of the photonic properties of graphene, other notable reviews are available on this subject and a few are listed here as a representative (but incomplete). Review articles describe: graphene photonics [3, 4, 5, 6], graphene electronics [7, 8], and plasmonics[9]. In addition, significant efforts in other two-dimensional materials, van der Waals solids, and heterostructures may be of critical interest as well [10, 11].

1.1 Relevant Material Properties

Graphene shows potential for ballistic carrier motion with an inferred mean free path $> 2\mu$m at room temperature [12], and has an extraordinarily high carrier mobility, $> 25,000$ cm^2/V·s, at room temperature. As a comparison, this is 3x (63x) higher than the room temperature electron (hole) mobility in bulk GaAs, and 17x (56x) higher than the electron (hole) mobility in bulk Si. These bulk, room-temperature carrier mobility values for GaAs and Si are often used for photodetectors. However, it should be noted that efforts have been undertaken to increase these values, for example in high-electron mobility transistors (HEMTs) and two-dimensional electron gasses (2DEGs). This work has resulted in low-temperature (~ 4 K) mobilities $> 10^7$ cm^2/V·s in GaAs heterojunction 2DEG [13, 14, 15].

Other physical features which make graphene of interest are its high thermal conductivity (10x copper and 2x diamond) and high electrical conductivity (100x copper), and high tensile strength (0.13 TPa, 100x that of steel). Another unique physical property of graphene is that it exhibits fractional quantum Hall effect due to the collective behavior of its carriers.

The optical properties of graphene are also fascinating, beginning with its universal optical conductance, $\pi\alpha$. This means that the optical conductivity is based upon the fine structure constant, α, which is equal to the physical constants $\frac{1}{4\pi\epsilon_0}\frac{e^2}{\hbar c}$ [mks], or equivalently ($e^2/2\epsilon_0 hc$) or ($e^2 c\mu_0/2h$) [16, 17], where e is the electron charge, h is Planck's constant, c is the speed of light in vacuum, and ϵ_0 and μ_0 are the permittivity and permeability of free space (respectively). This provides graphene with the interesting optical property of broadband (visible – IR) linear absorption of 2.3% per monolayer.

Manuscript approved June 3, 2014.

As an optical absorber, graphene has a high-damage threshold (10 mJ/cm^2) [18]. This is similar to the damage threshold of silicon for similar optical pulse parameters [19]. However, silicon has a 10-μm absorption depth (at these wavelengths) which causes 2.3% of the light to be absorbed in a 200-nm thickness as opposed to the same optical absorption in a much smaller 0.3-nm thickness (interplane spacing) of graphene. Thus, with a similar damage threshold graphene should have a larger density of excited carriers than in silicon. For example, using linear absorption a 1000x higher carrier density is created in graphene vs. silicon.

Other notable optical properties include nonlinear optical properties of saturable absorption [20], photoexcited hot-carrier dynamics, and optical parametric conversion. The utility of graphene extends to plasmonic properties that stem from its two-dimensional electron gas (2DEG) and strong surface plasmon polariton (SPP) coupling in the visible and near IR. Finally, graphene's demonstration as a THz transistor shows potential in high-speed electronics/photonics.

1.2 Fabrication

Graphene fabrication is the necessary first step not only in creating graphene but also in determining its viability for mass production of devices. Graphene may have first been created by Edward Acheson in the 1890's while processing carborundum (SiC), although the graphene was unidentified [21]. More recent (and Nobel prize winning) attempts achieved graphene via mechanical exfoliation in 2004 [2]. This process can produce graphene with extremely high carrier mobilities $> 200,000$ cm^2/V·s at room temperature. Unfortunately, these films have a very small area (100 μm^2), and this makes it expensive ($10M for 1cm^2) for industrial applications. Also in 2004, a large-area process of epitaxial graphene on SiC was created (similar to Acheson) [22]. These have been scaled to larger than 4" wafer sizes and exhibit high room temperature carrier mobilities, $25,000$ cm^2/V·s [23]. [Note: while this mobility is about 8x lower than the highest quality exfoliated pieces, it is still 3x (63x) higher than the electron (hole) mobility in bulk GaAs.] Other industrial scale graphene can be produced by chemical vapor deposition (CVD) to create graphene on copper and nickel foil sheets, thereby producing inexpensive, large area (30" rolls) [24, 25] at the expense of lower quality graphene with (for example) lower carrier mobility.

While these are the most popular, several other methods exist including graphite oxidation and subsequent graphite-oxide reduction, liquid phase sonication and exfoliation, as well as electric arc graphene production [26]. In addition, methods have been developed for transferring graphene films to other substrates [27]. This allows implementation on a wider variety of substrates and increases graphene's application by allowing operation on (and interaction with) various semiconductors, insulators and metals.

1.3 Graphene's potential: carbon-based electronics and photonics

Graphene boasts the potential for ballistic carrier transport, i.e. its carriers propagate via diffraction (like optical light in a waveguide), rather than by carrier diffusion as is common with carriers in conventional semiconductors. This potential for ballistic transport along with graphene's other electronic transport properties spark an interest for its use in carbon-based electronics. Processing graphene into devices can be achieved by conventional Si-fabrication technology. In addition, due to its thickness and material properties, graphene is flexible, and (as previously mentioned in the fabrication section) can be transferred to other substrates. This enables a graphene coating on optics and other structures. Thus, graphene's mechanical, electronic, and photonic properties can be exploited on nearly any substrate. These graphene-based designs can be extended to autonomous, self-powered devices by using graphene as a photovoltaic solar-cell.

Together with its remarkable optical properties of a broadband response from the UV through THz, high-speed photodetection can now be achieved on any substrate or object by transferring a graphene film. Graphene devices have been fabricated for use as nonlinear optical and photonic devices: such as for sat-

urable absorbers, optical modulation, optical gating, to name a few. Recently, an all-graphene photonic integrated circuit was demonstrated using plasmonics [28]. The potential of this material in photonics is only beginning to be realized. The next section will examine graphene's current and potential uses in photonics.

2 Graphene Photonics

As with electronics, the present and future of photonics seems to be shrinking, namely, in device size. In this paradigm, two-dimensional graphene is showing future promise in these devices and systems. For high-speed optoelectronic devices graphene's high-carrier mobility [16] is a benefit. Applications in a variety of spectral regions will gain from graphene's broad spectral absorption [17]. For applications requiring robust photonic and nonlinear optical structures graphene's high optical damage threshold [18] and mechanical strength [29] will be paramount. In addition, the ease of graphene's transfer to other substrates and its ability to conformally coat surfaces make it ideal for integrating hybrid photonic systems.

This section aims to provide a basic understanding of graphene's use in photonic devices. This is broken into five parts: 1) Photodetection, 2) Electro-optic modulation, 3) Optical polarization, 4) Plasmonics, and 5) Nonlinear optical properties and devices.

2.1 Photodetectors

Three main categories of photodetectors have been created using graphene. In the first category photons couple to electrons producing an electronic response, which describes photovoltaic style detectors. A second category involves coupling photons, electrons, and phonons and results in hot-electron bolometers. Finally, a third embodiment utilizes a hybrid graphene photodetector: one material absorbs light (e.g., quantum dots) and is integrated onto graphene to exploit graphene's carrier collection and transport properties.

In Figure 1 some of the graphene photodetectors discussed in this section are compared with each other as well as with commercially available photodetectors. Responsivity is used as a figure of merit for comparison with telecommunications. However, responsivity is a function of wavelength ($R = \eta\lambda/1240$ [A/W], for λ in [nm]), thus, a dotted line denoting a 100% quantum efficiency ($\eta = 1$) adds a reference for this spectral comparison. Fast graphene photodetectors have responses ≤ 1 ns and are denoted with a red color, while those in blue represent slow responses of ≥ 1 second. The commercial photodetectors (Si, Si APD, and InGaAs) all have fast responses ≤ 1 ns. The following sections describe each of the three styles of graphene photodetectors (photovoltaic, photothermal, and hybrid) in detail.

2.1.1 Photovoltaic Detectors

An amazing aspect of graphene is its large absorption of light over a broad spectral bandwidth (from the ultraviolet to the far infrared. For it's 0.33-nm monolayer thickness it absorbs roughly 2.3% of the incident light. This makes it 10-1000x more absorbing than semiconductors, such as Si and GaAs, while covering a much broader spectral bandwidth. These properties make graphene potentially attractive as a photovoltaic solar cell [30]. Furthermore, a thin and flexible graphene solar cell can also be transferred onto a variety of substrates such as optical lenses and mirrors [27, 31].

While absorption in graphene is large for a monolayer, graphene still transmits 97.7% of the incident light. Unlike most materials, graphene forms in a continuous monolayer. Thin metals (e.g. conductors like Au, Ag, etc.) do not form a continuous layer, instead forming into islands that eventually connect once an average thickness of about 10 atomic layers are deposited. Thus, graphene's continuous monolayer makes

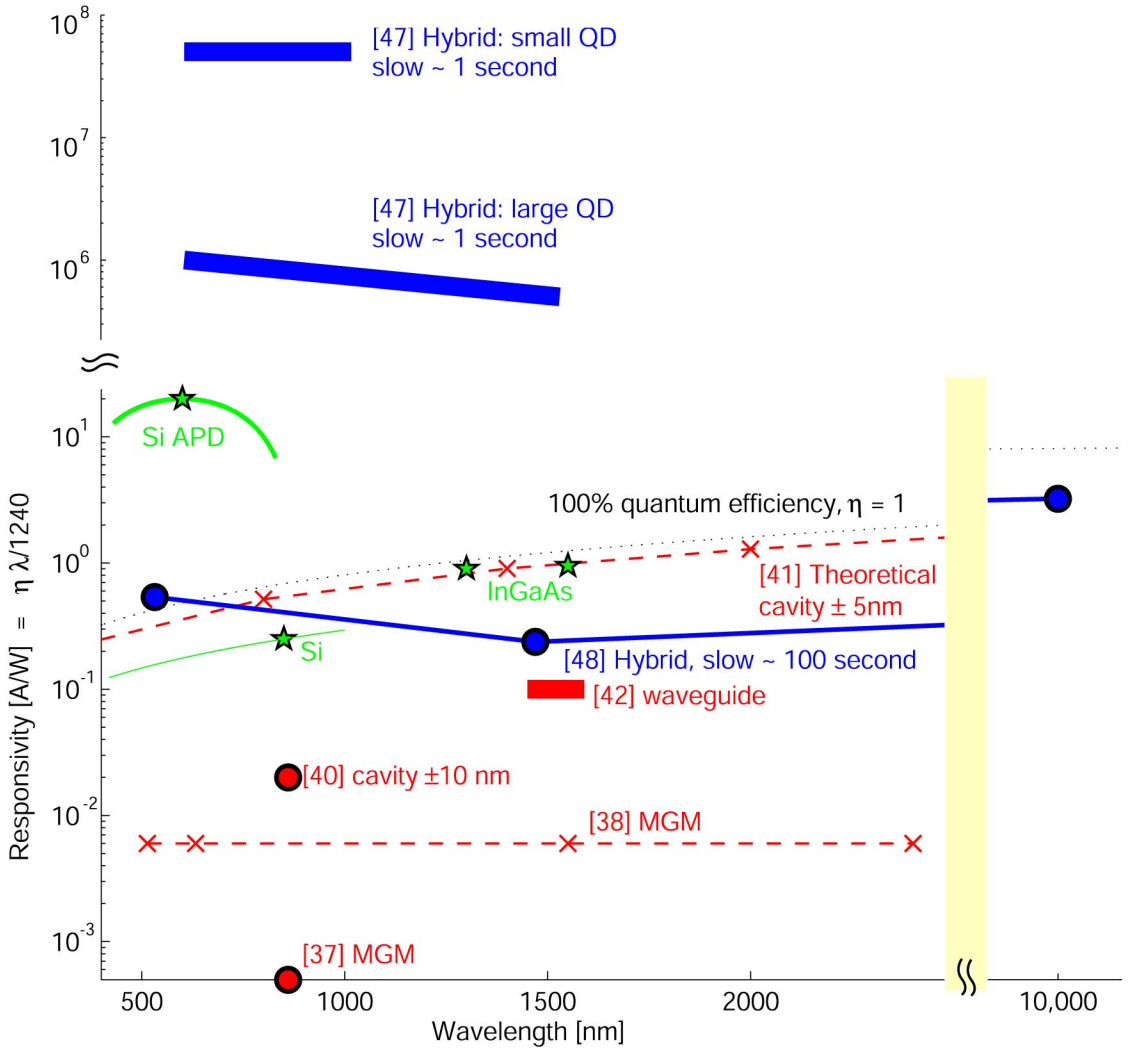

Figure 1: Spectral responsivity of graphene photodetectors compared with commercial photodetectors. Dotted line shows 100% quantum efficiency, $\eta = 1$, as a function of wavelength. Red and green colors denote $\leq$ 1-ns response times, while the blue color denotes $\geq$ 1-second response times. The graphene photodetectors are labeled with their reference number [in brackets] as well as a brief description of the photodetector style: planar MGM (metal-graphene-metal), optical resonant cavity, waveguide device and hybrid graphene photodetector. The commercial photodiodes, shown in green, are Hamamatsu models S9055 (Si), S8664 (Si APD–avalanche photodiode), and G8195 (InGaAs).

it valuable as a optically transmitting electrode. Furthermore, graphene monolayers are extremely durable, with a 1-TPa Young's modulus and 0.13-TPa ultimate tensile strength (100x that of steel) [29]. As a robust, conductive, continuous monolayer that can be transferred to other materials, graphene has shown increased performance as a transparent (97.7%) electrode replacement for indium tin oxide (ITO) in solar cells [32].

In addition to detecting continuous light, photodetectors are also needed for measuring pulses of light. For detection of picosecond and subpicosecond optical signals, photovoltaic detectors are frequently made from materials with high carrier mobilities. Often there are tradeoffs between mobility and efficiency. For example, GaAs has high-mobility electrons but suffers from much lower mobility holes which limit the device speed. To achieve higher speed operation unitraveling-carrier devices effectively remove the hole response [33]. Similarly low-temperature grown materials effectively trap the slower carriers [34, 35], at the

cost of reduced collection efficiency, although this can be mediated by a geometry using the low-temperature material as a gate [36].

In graphene, several high-speed photovoltaic detectors have been created. Detection of 40-GHz waveforms has been demonstrated with single layers of graphene [37]. An upper limit of 500-GHz was predicted after measuring the device's parameters, although the fabricated device and measurement system limited the tested device to 40 GHz. A high-speed graphene photodetector was fabricated using standard design and lithographic processing used in high-speed metal-semiconductor-metal (MSM) photodiodes, in this case a metal-graphene-metal (MGM) detector (see Figure 2). This device showed digital telecommunication operation of 10-Gbit/s at 1550nm [38].

Unlike the complex vertical growth needed for p-i-n photodetectors, the planar fabrication used in the MGM detectors makes this design very easy to implement by merely substituting graphene for the semiconductor photon absorber. Unfortunately, this is not an ideal geometry for an efficient graphene photodetector for a number of reasons. Graphene is a semi-metal (not a semiconductor) and it absorbs only 2.3% of light per monolayer, which is large for a monolayer but inefficient for a photodetector. In addition, the process for collecting the photogenerated electrons is lower than expected [39] and more work is needed to understand the physical mechanisms involved. To improve carrier collection, several groups have experimented by varying the work function of the metal contacts to increase collection of the photo-generated electrons [39].

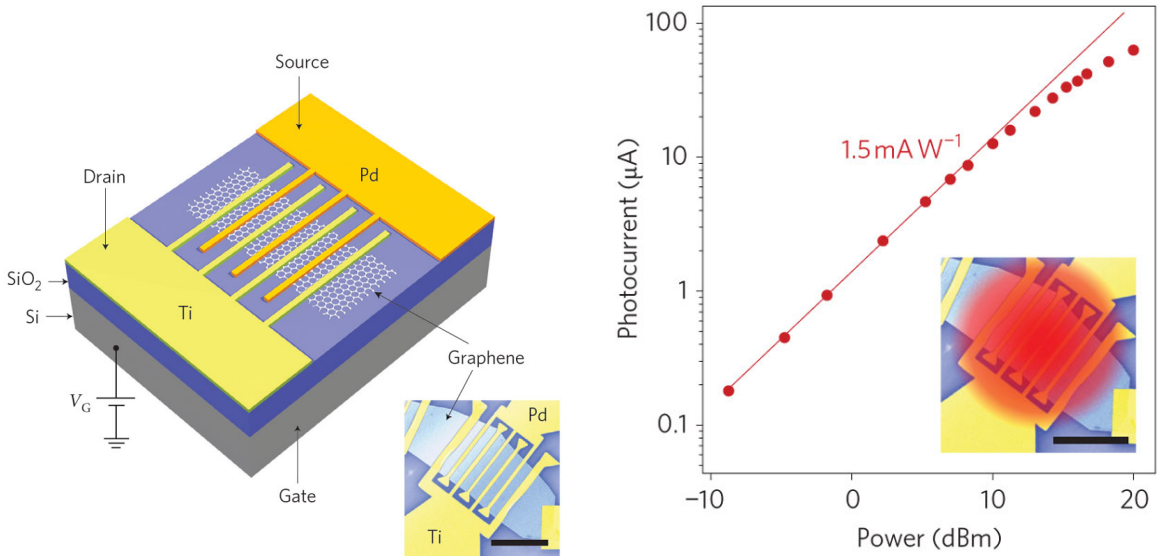

Figure 2: MGM photodetector drawing and fabricated structure along with its photocurrent response at 1550nm (from [38]).

Responsivity is a measure of the electrical output for a given optical input. The maximum responsivity varies with wavelength (λ) and with the conversion efficiency of photons to detected electrons (or quantum efficiency, η), and is described by the equation $R = \eta\lambda/1240$ [A/W], for λ in nanometers. Thus, assuming 100% quantum efficiency, the maximum responsivity $R_{\text{max}} = 0.69$ A/W at $\lambda = 860$nm, and $R_{\text{max}} = 1.25$ A/W at $\lambda = 1550$nm.

While these MGM detectors have incredibly broadband spectral detection (graphene absorbs in the UV, visible, near and far IR), these MGM style detectors have low responsivity due to the 2.3% monolayer absorption. Responsivity improvements using resonant-cavity enhanced (RCE) detectors have improved the MGM's 5×10^{-4} [37] A/W to 0.02 A/W (at 860nm) [40] (see Figure 3). RCE devices, however, reduce the broadband optical detection, in this case to about ± 10 nm, full-width at half maximum (FWHM).

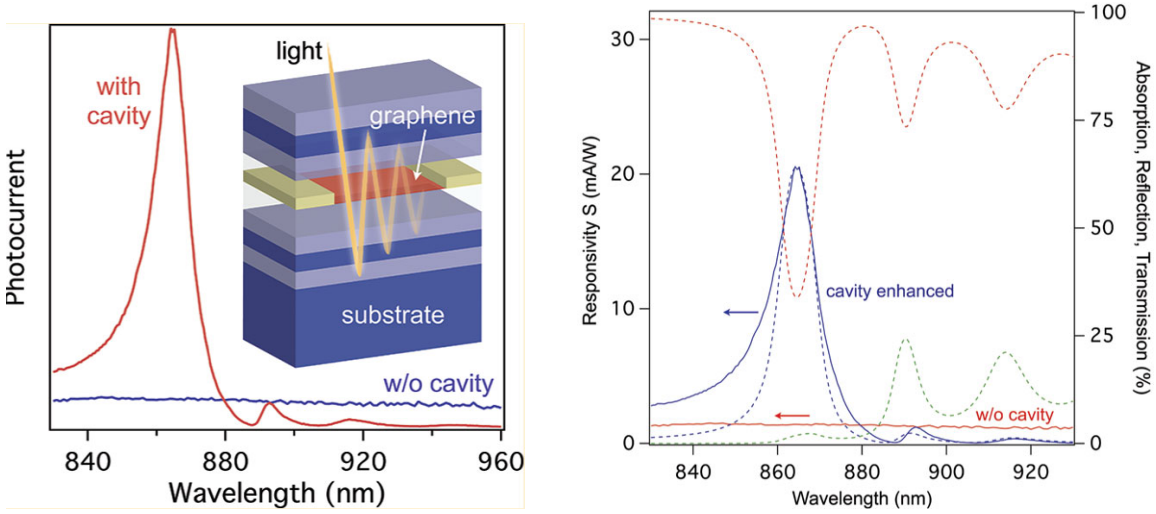

Figure 3: A graphene microcavity photodetector traps light using distributed Bragg mirrors in a multipass cavity containing graphene. This cavity multiplies the absorption of a single graphene layer, thereby increasing responsivity at the expense of the cavity's spectral bandwidth (from [40]).

Ferreira *et al.* predict 100% absorption by employing two optical cavities [41]. The predicted absorption is not for the 100% of the incident light, but only for the light which is coupled into the optical system. This optimized two-cavity system is comprised of a half-wavelength cavity coupled to a quarter wavelength cavity, although this significantly restricts the spectral bandwidth to about ± 5 nm FWHM [41].

Another method for increasing the responsivity is to place the graphene on an optical waveguide and then couple the waveguide's evanescent field into the graphene. This waveguide detector provides large (100 μm) interaction lengths in comparison to the monolayer interaction lengths of in the MGM and RCE based detectors. The optical waveguide limits the optical spectrum (similar to RCE devices) to the modes guided in the optical waveguide, as well as to those modes whose evanescent field strongly couples to the graphene.

In addition, high-speed operation requires group-velocity matching of the optical and electrical signals. Gan *et al.* have demonstrated a $>$ 20-GHz waveguide photodetector (see Figure 4) with a responsivity exceeding 0.1 A/W over a range of wavelengths, from 1450 to 1590 nm [42]. The calculated graphene absorption from Gan *et al.* was approximately 0.08 dB/μm, and the optical loss coupling into the waveguide was $>$ 3dB. These waveguides need strong evanescent-field coupling to the graphene, so they often employ sub-micron dimensions which requires more complex fabrication and optical coupling. This can lead to high optical insertion losses. In addition, the broad optical absorption spectrum of graphene is limited to those optical wavelengths that are guided in the waveguide.

2.1.2 Photothermal Detectors

Bolometers are at the heart of photothermal detection. In bolometry, the absorption of incident photons is converted into a change in temperature, often observed by a change in the material's resistance. A bolometer usually employs a small mass to absorb the incident energy. This small mass is coupled to a larger mass, the thermal bath, creating a temperature difference between the two masses. This difference is controlled by the smaller mass's thermal capacity as well as by thermal conductance linking the small mass and the thermal bath. Several methods of thermometry can detect the rise in temperature, and thus the quantity of absorbed radiation. Bolometers can be made from metals, semiconductors and superconductors, and usually have their optimal performance at low temperatures.

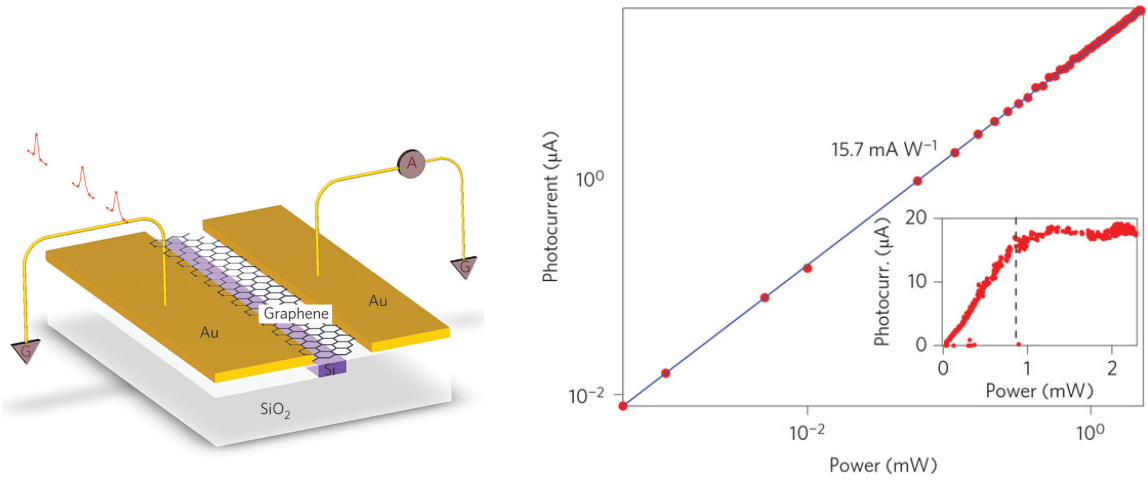

Figure 4: A silicon waveguide detector uses a graphene film on top the waveguide as an absorber and achieves an increase in photocurrent over normally-incident photodetection by effectively increasing the photodetection volume by increasing the length of the waveguide. (from [42]).

Instead of using two discrete masses, bolometers can use electron and phonon temperatures as the two coupled systems. These are known as hot-electron bolometers and the coupling between the two systems is linked by electron-phonon coupling. Under optical excitation, photo-excited carriers gain energy and relax by radiative and nonradiative mechanisms. In the non-radiative mechanism the excited carriers can transfer this energy to the phonons through electron-phonon coupling. This happens on picosecond time scales.

In graphene, as in semiconductors, there is a fundamental difference in carrier dynamics between *cw* and pulsed optical excitation [43]. When photons are absorbed in a material, their energy is transferred to the electrons and phonons. An equilibrium condition in the material can be represented by demonstrating that the electron and phonon subsystems are at the same temperature, and are also at the same temperature as the substrate. Nonequilibrium conditions can exist in which the electron and phonon subsystems are not in equilibrium with each other and/or not in equilibrium with the substrate. These are referred to as hot-electrons or hot-phonons to indicate that these subsystems can be represented by an elevated temperature with respect to the substrate. Energy transfer occurs between the subsystems and substrate to equilibrate the system. These non-equilibrium conditions usually exist only for short times (e.g., femto- to pico-seconds) before equilibration. Thus, the nonequilibrium conditions are exacerbated by short optical pulse excitation. Excitation with *cw* light causes only a small increase in electron temperature, while pulsed optical excitation causes a dramatic increase in the carrier temperature, > 1000K above the lattice [44]. Hot-carriers generated by pulsed excitation will decay via optical and acoustic phonon cooling.

A hot-electron bolometer was recently created with graphene. As the name implies, this device exploits the electron temperature. Hot-electron bolometers usually work in non-equilibrium excited-carrier regimes in which the electron, phonon and substrate temperatures are not in equilibrium. In graphene, the rapid absorption of light in the electronic system combined with the weaker electron-phonon coupling allows a large non-equilibrium temperature between the electron and phonon subsystems. This is enhanced by the low electron heat capacity in graphene. The change in resistance as a function of the electron heating was measured in bilayer graphene (see Figure 5), and produced a voltage responsivity of 2×10^5 V/W with a noise equivalent power of 33 fW Hz$^{-1/2}$ at 5K [44]. This hot-electron bolometer had a sub-nanosecond temporal response (0.1-0.25 ns). These features make this device competitive with commercial silicon bolometers.

To this point, graphene has been assumed to be a simple semimetal absorber. The Fermi level is assumed to be at the Dirac point in the band structure. However, the Fermi level can be moved to dope the graphene to

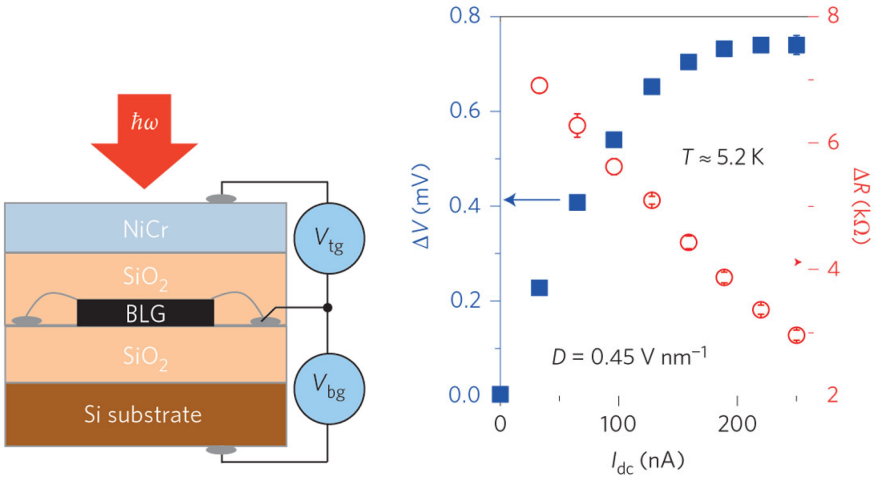

Figure 5: Drawing of a bilayer graphene hot-electron bolometer with dual gating along with its response to ~ 4 μW of 10-μm-wavelength incident light showing a voltage responsivity of 2×10^5 V/W, (from [44]).

make it either p- or n-type. High-speed photodetectors can be created by making p-n junctions in multilayer graphene. By creating a p-n junction in graphene, Sun *et al.* used pump-probe spectroscopy coupled with scanning photocurrent microscopy to evaluate the effects of optical phonon, Peltier, and acoustic phonon cooling (see Figure 6). This technique indirectly measured a 1.5-ps temporal response (at room temperature) caused by hot-carriers (rather than phonons) in multilayer graphene with p-n junction photodetection [43]. This provided a fast graphene photodetector based on the p-n junction rather than the metal-graphene-metal type of photodetector previously mentioned in the *Photovoltaic Detectors* section.

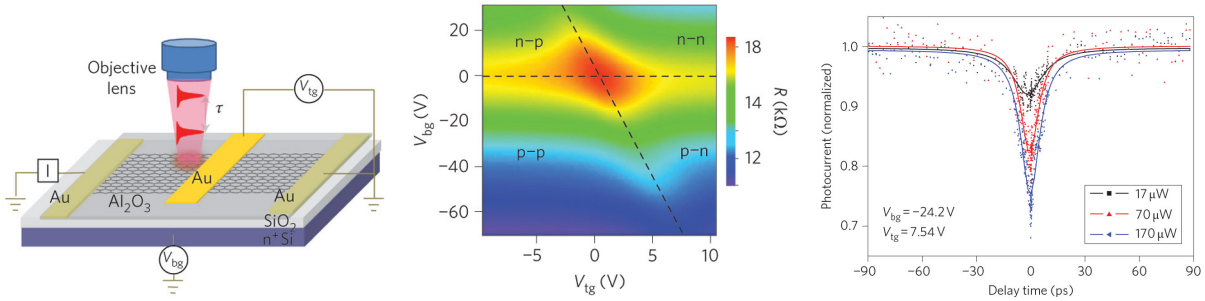

Figure 6: Schematic of a graphene hot-electron bolometer by applying top and back gate voltages to create a tunable graphene homojunction whose configuration (n-p, n-n, etc.) is shown as a function of top and back gates. A picosecond signal is demonstrated in response to an applied 250-fs optical pulse. (from [43])

Recently, Fong and Schwab directly measured the electron-phonon coupling in graphene and determined the heat capacity of graphene's 2D electron gas [45]. From these measurements, they estimate a temperature resolution limit determined by the thermodynamic fluctuations of the energy of the electron gas. An estimated sensitivity on the order of 10^{-20} W Hz$^{-1/2}$ is claimed for these devices at low temperature [45]. In addition, the rapid thermal time constant could provide a 10^5 bandwidth improvement over current detectors. While 10x less sensitive than new superconducting photon counters, a 7x energy resolution is expected making graphene a potential low-flux THz photon counter [45], based upon concepts of Karasik and Sergeev [46]. With these attributes, graphene has potential for far-infrared or submillimeter-wave astron-

omy, with the possibility of photon counting at frequencies as low as 800 MHz, thus, enabling exploration of quantum experiments with microwave photons [45].

2.1.3 Hybrid-graphene photodetectors

In the previous photodetection methods, graphene was used as an absorber in the photodetector. However, recent hybrid photodetectors have used another absorbing medium while using graphene to collect and transport the photo-generated carriers. For example, a thin film of colloidal quantum-dots, with strong and tunable light absorption, cover a graphene monolayer (see Figure 7). Graphene's high-mobility together with the trapped-charge lifetimes in the quantum-dot produced a photodetector responsivity of 10^7 A/W [47].

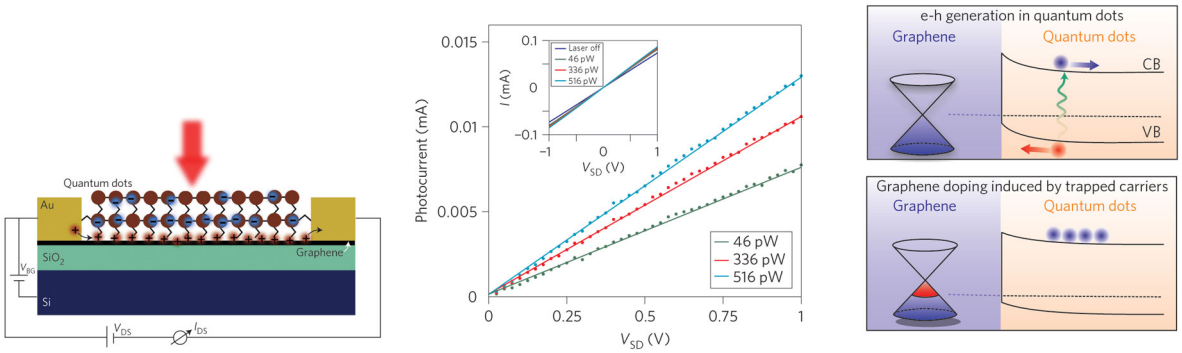

Figure 7: A hybrid photodetector using PbS quantum dots as the photodetection transducer changing incident light into mobile carriers. As shown in the energy-band diagram, electrons are trapped in the dots while holes are transferred to the graphene and produce a photocurrent (from [47]).

In another example a monolayer of graphene is coated with titanium that is processed into a graphene quantum-dot-like-array and mid-gap states are formed for carrier trapping. This produces a responsivity of 8.61 A/W in a relatively broadband photodetector (visible to near-IR) due to impact ionization in the quantum dots and the long lifetime of the traps [48]. In this case, the demonstrated operation speed is slow ($<$ 10 Hz), and photocurrents are $<$ 200nA, however, the high responsivity makes this a useful device for measuring low-level broadband signals.

Research is underway to functionalize graphene's surface with other elements and molecules. As hybrid photodetectors, these designs may begin to form a gray area between photodetectors and sensors.

2.2 Electro-optic Modulation

Modulation of light is needed in many photonic applications. Materials can be used for electro-optic modulation of light if some characteristic of the light (amplitude, polarization, etc.) can be modified by an applied electric field or injected current. Electro-optic modulation is commonly achieved by several popular methods, such as 1) an electro-optic material (electric-field terms of a material's nonlinear susceptibility), 2) an electro-absorption material (absorption characteristics are electrically modified), 3) electrically induced modulation of an optical material's refractive index (e.g., electric field or current injection modifies carrier density producing a carrier-refraction effect), 4) electrically induced thermal variations which modify an optical material's properties.

A graphene-based electroabsorption (EA) modulator was experimentally demonstrated by depositing a graphene monolayer on an optical waveguide [49]. The highly-confined optical field in the Si/SiO waveguide interacted with the graphene and oxide cap through the evanescent field (see Figure 8). An electric field has been shown to modify the conductivity, electron-phonon coupling, work function and Fermi level in

graphene [2, 50, 51]. Liu *et al.* used an electric field to tune the Fermi level of a graphene sheet, thereby, changing the optical conductivity/absorption and creating an optical modulator [49]. Through this technique they obtained an electroabsorption modulation of 0.1 dB/μm, demonstrating a device with a small footprint (25 μm^2). Greater than 1-GHz modulation frequency was obtained over a broad optical bandwidth (1.35-1.6μm). In addition, the modulation was polarization sensitive since the graphene interacts only with the in-plane electric field of the evanescent optical wave.

EA modulators are common in optical telecommunications as they often operate with a lower voltage bias than those modulators made with electo-optic materials. The operation of EA modulation is often achieved by shifting absorption energies, usually in semiconductors and quantum-confined structures by employing the Franz-Keldysh or Quantum-confined Stark effects. One drawback of EA modulators is their absorbed optical power can limit device operation. However, graphene's high thermal conductivity may overcome this potential limitation by rapidly carrying the heat away from the device.

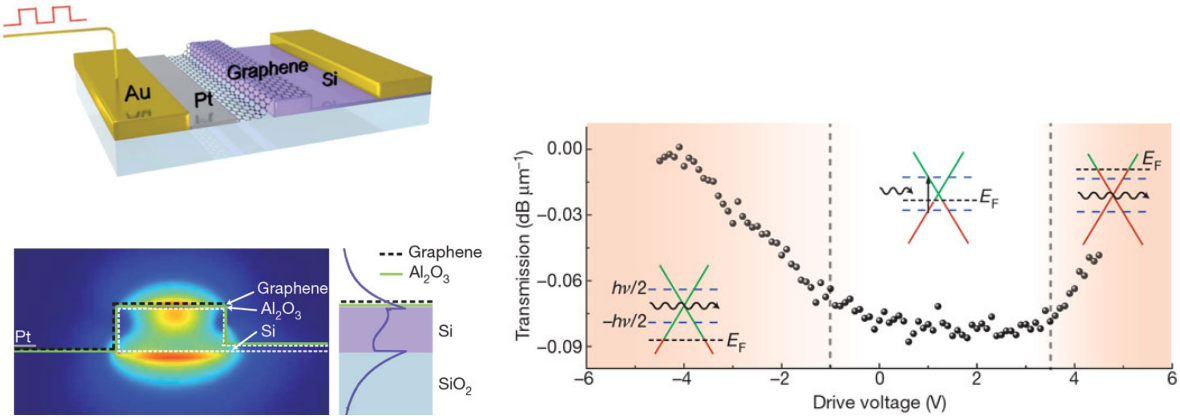

Figure 8: Schematic diagram and cross section of the optical mode in an graphene-based EA modulator along with a plot of the E-field modulation of optical transmission with the energy-band diagrams explaining the field-induced shift in Fermi level, E_F (from [49]).

In another recent experiment, the optical transmission of graphene was modulated using coplanar electrodes on multilayer graphene [52]. This simple experiment merely placed a voltage between the electrodes and measured a small (few percent) change in the optical transmission over a broad optical bandwidth (visible region). The modulation was slow (on the seconds time scale) and allows higher harmonics of the modulation frequency through. Further work is needed to understand the physics of this effect, however, it is such a simple concept that it may be widely applicable.

Another method for light modulation was recently demonstrated using reflection in the mid-infrared and THz region. By applying a magnetic field on multi-layer graphene structures, the inter-layer coupling was investigated by polarization-sensitive magneto-optic Kerr spectroscopy [53]. The experiments observed cyclotron resonant Kerr features that demonstrated optical reflection induced by an external magnetic field. The understanding gained from this experiment suggests the potential for replacing the external magnetic field with an electrostatic gate [53].

All of these discoveries in electrically-induced light modulation by graphene have occurred within the past few years. This may be only the beginning for unlocking the potential of electrically-induced light modulation by graphene.

2.3 Polarizers

Applying graphene on top of optical waveguides allows the optical field to evanescently couple to the graphene. This was mentioned earlier in the both the waveguide-based graphene photodetectors as well as the waveguide-based graphene electroabsorption modulator. The same method is used (without an applied electric bias) to create an optical polarizer. The polarization (as discussed earlier) arises only from graphene interaction with the in-plane electric field of the evanescent optical wave. This technique was demonstrated in a single-mode optical fiber which had been polished to the fiber core producing a flat region upon which the graphene was transferred [54]. The propagation distance, L_G, was defined as the length of covered by the graphene film. At a wavelength of 1550 nm, increasing L_G from 2 to 7 mm caused polarization extinction ratios to increase from 22 to 27 dB. The measured polarization extinction from monolayer graphene was nearly the same as when few-layer graphene was deposited on the fiber. Polarization over a broad spectral bandwidth (from 400-2000nm) was obtained (see Figure 9). TE and TM coupling to and absorption by the graphene was discussed as the waveguide's polarization mechanism, with a maximum polarization extinction ratio of 27 dB [54].

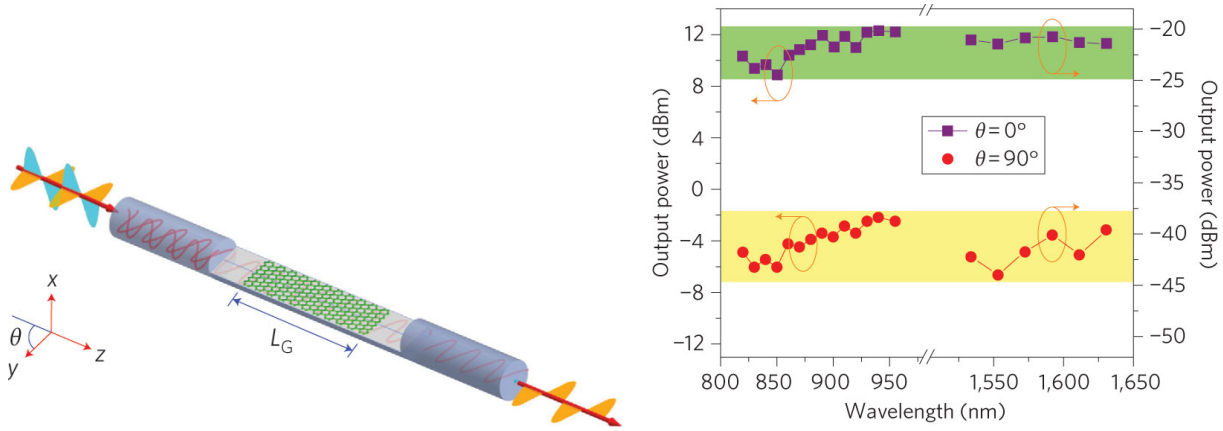

Figure 9: Schematic diagram of the polished fiber with graphene (L_G = 2–7 mm) laid across the core and a plot of the transmitted polarization as a function of wavelength (from [54]).

Other graphene-based optical polarizers have been created by coupling to surface plasmon polaritons (SPP) in the graphene. In one case, an attenuated total reflectance geometry was considered with graphene at the total-internal-reflective surface [55]. When a resonance condition is met between the incident electromagnetic (EM) wave and the polariton mode in graphene, then a SPP is excited in graphene and the reflectivity of the EM wave is reduced. The coupling of both TE and TM polarization are possible depending on the imaginary part of the complex conductivity for the effective dielectric material surrounding the graphene. In addition, the position of the Fermi level in graphene can influence this coupling, so adding a voltage bias to the graphene may allow tuning of the polarizer. The degree of polarization can then be controlled by varying the applied voltage. The authors mention the use of this for a tunable polarizer in the THz frequency range [55], however, it could also be possible to use this as a THz modulator. Finally, since this is a theoretical study it is potentially applicable to optical frequencies with appropriate dielectric materials.

2.4 Plasmonics

Plasmonics have the ability to couple light into nano-structures that are smaller than 1/10 of the wavelength of light. This is very attractive since it affords the opportunity of light and matter interactions on a deep

sub-wavelength scale. For photonics this allows integration of light and electronics, enabling plasmonic lenses [56], focusing to the nanoscale [57], and engineered metamaterials [58]. In addition, the confinement allows electromagnetic field enhancements and can provide extraordinary nonlinear optic and electronic phenomena [59].

Plasmas are many-body carrier effects which arise through resonant collective oscillations of lightly damped carriers. These effects can occur in free-electron systems: gases (ionization and conduction in discharge tubes, e.g. Neon), metals, and doped semiconductors (highly doped and/or inversion layers). In graphene, quantized plasma modes (plasmons) are confined to the surface and interface between the graphene and the surrounding dielectric, thus, surface plasmons are considered. The coupling of light with the 2D carriers can be described by surface plasmon polariton (SPP) (the term polariton derived from, "coupled electric ***polari***zation-pho***ton*** waves"[60]). Depending on the material, the "light" ranges from THz to UV wavelengths, so this is attractive for many areas of photonics including sensing, imaging, and communication.

Graphene has unique properties which make it a useful plasmonic material. As a semi-metal, graphene's carrier concentration can be changed (unlike metals). This provides an opportunity for tuning the plasmon resonance. For example, an applied gate voltage could be used to tune the carrier concentration, thereby tuning the plasmonic behavior [61].

In addition, graphene's carriers are confined to two-dimensions, however, this 2D system lives in a 3D world and therefore adjacent dielectric materials influence its response. This can be used in addition to the (previously mentioned) gate voltage to tune the plasmon resonance. In addition, epitaxial graphene on SiC shows dramatically different behavior than that of suspended graphene [62]. This is explained by the high doping of graphene caused by the SiC substrate which influences (through contributions to the electronic dispersion) the coupling between the graphene's plasmon and SiC's surface optical phonon.

The massless Dirac fermions in graphene have a linear electronic dispersion, but graphene's plasmons have a nonlinear dispersion relationship. Long-wavelength plasmons in a Dirac system have a frequency proportional to $1/\sqrt{\hbar}$ in all dimensions (1D, 2D, or 3D) [63]. This is a non-classical result and differs dramatically from the long-wavelength plasmon frequency in a classical two-dimensional carrier system. In addition, the plasmon frequency in graphene exhibits a fourth root carrier density dependence ($\omega_0 \propto \sqrt[4]{n}$), as opposed to the square root dependence in other two-dimensional electronic systems [64]. Besides their differences there are similarities to classical plasmons. One example is that graphene's long-wavelength plasmon dispersion is proportional to the square root of the wave vector ($\omega = \omega_0\sqrt{q}$), as shown in Figure 10 where at low-energies (long-wavelengths) the dispersion matches the quadratic dependence of the Drude model (shown as dashed lines).

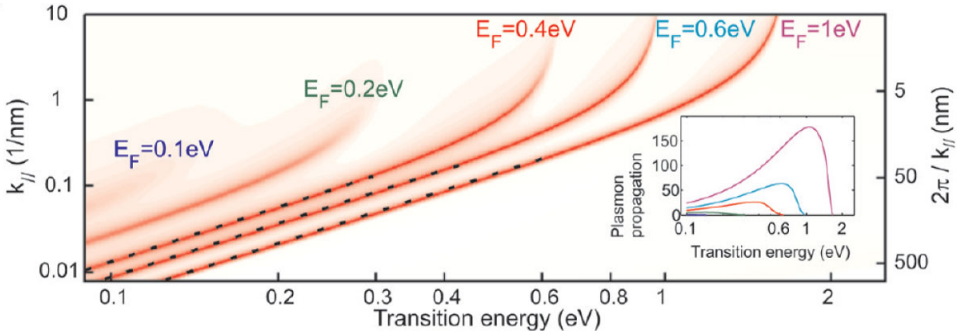

Figure 10: A contour plot illustrates plasmon dispersion in doped graphene. The contours show the magnitude of the Fresnel reflection coefficient as a function of Fermi level. These demonstrate the quadratic dependence on plasmon energy with the dashed lines corresponding to Drude model. The inset shows the propagation distance, in units of the surface plasmon wavelength (from [65]).

Unlike plasmons in metals which tend to be lossy with resonances confined to the visible and UV, graphene's properties allow lower losses and operation in the infrared and THz [58, 65]. This is due (in part) to graphene's tight confinement of the surface plasmon polariton guided mode. This attribute enables a large ratio of the plasmon wavelength to the free-space wavelength, and enables long plasmon propagation lengths [58]. For example, a 10-μm free-space wavelength (30 THz) can couple to a graphene SPP of 144-nm wavelength, representing a 69x compression in size of the free-space-optical mode to SPP-guided mode. Also, the propagating length of this guided SPP, defined by the imaginary part (loss) of the SPP wavenumber, is 2.25μm, which represents 15.6x its SPP wavelength [58]. This length is long enough to create plasmonic devices, while also ensuring isolation between adjacent devices.

Based-upon these fundamental properties, a variety of applications have been devised utilizing graphene plasmonics, such as optical polarizers, optical modulators, and photodetectors. This was previously mentioned in the case of the of tunable polarizer, where electro-magnetic waves coupled to graphene's SPP [55].

Plasmonic resonances in the mid-infrared, 900-2500 cm^{-1} (4 to 11 μm) were observed by creating graphene nano-structures. Nanoresonators were fabricated in the mid-infrared using 15- to 80-nm width graphene structures formed into arrays [66]. The experimental results provided the ability to calculate the dispersion relations of graphene plasmons in this mid-infrared spectral region. In addition, graphene's charge density was altered by applying an external voltage bias to these back-gated structures, and this created another mechanism (besides adjusting graphene's width) for altering the plasmon resonances [66]. The shifting of plasmon energy as a function of width and applied bias are shown in Figure 11.

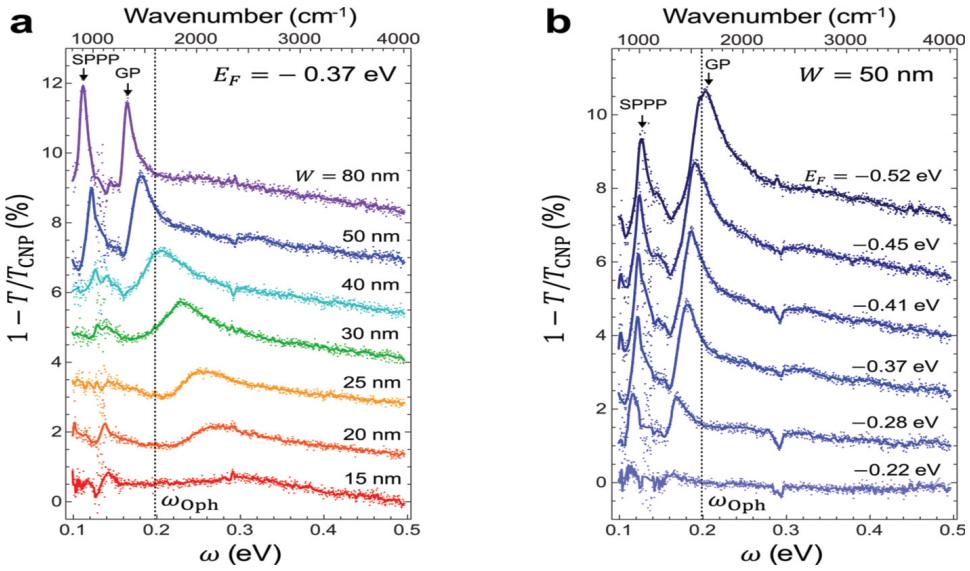

Figure 11: Optical transmission through graphene plasmonic nanoresonator arrays show both surface plasmon phonon polariton (SPPP) and graphene plasmon (GP) peaks. The vertical axis represents the change in optical transmission normalized to the optical transmission at the Dirac point, or charge neutral point (CNP). The position of the resonances change as a function of (a) resonator width, and (b) applied back-gate bias, shown here as a shift in the Fermi level of graphene, for a 50-nm wide structure (from [66]).

Another graphene plasmonic system was published earlier this year demonstrating an all-graphene photonic integrated circuit [28]. Normally graphene is integrated with semiconductors to produce photonic circuits, but in this case only graphene is used. A polymer coated substrate is used as a base to support the graphene. The incident 1550-nm light is coupled to a graphene plasmonic waveguide, and is guided to a graphene photodetector. The system only shows an $\sim$ 40-ms time response, however, this is the first all-

graphene photonic integrated circuit [28]. This demonstration provides impetus for a new class of low-cost, 2D photonic integrated circuits.

2.5 Graphene as a Nonlinear Optical Device

Graphene possesses a nearly wavelength independent linear absorption from the visible through the far infrared while absorbing a large amount (2.3%) of light per monolayer [17]. With a finite number of quantum states in the monolayer, graphene exhibits a nonlinear saturation of its optical absorption at relatively low saturation intensities [20]. This is due to the Pauli exclusion principle, which allows only two Fermions (spin up and spin down) to simultaneously occupy a single quantum state. Thus, by Pauli's principle potential absorption pathways are blocked producing a saturation of the absorption, thereby making graphene more transparent (less absorbing) under high optical irradiance. This saturable absorption effect is well known in nonlinear optics, but occurs at a low-threshold for graphene, due to graphene's large optical absorption coefficient. This effect in graphene was first experimentally demonstrated in 2009 and was used as a mode-locking element for a fiber laser [67].

Degenerate femtosecond optical pump-probe spectroscopy utilizes two optical pulses of the same wavelength with a large-fluence pump pulse and a time-delayed lower-fluence probe pulse to measure a temporal change in material properties. To measure the temporal behavior of the saturable absorption in graphene 800-nm-wavelength, 100-fs optical pulses were applied in a degenerate optical pump-probe experiment. Before the pump pulse arrived there was no change in transmission of the probe pulse, but for $<$ 100-fs during the application of the pump pulse the graphene sample increased its transmission by 2% when subjected to a 25-pJ (9 MW/cm^2) pump pulse, Figure 12. Graphene's recovery to the steady-state transmission is described by a 0.15-ps exponential decay. Measured saturation intensities of 0.6 to 9 MW/cm^2 are common for multilayer graphene saturable absorbers [67, 31].

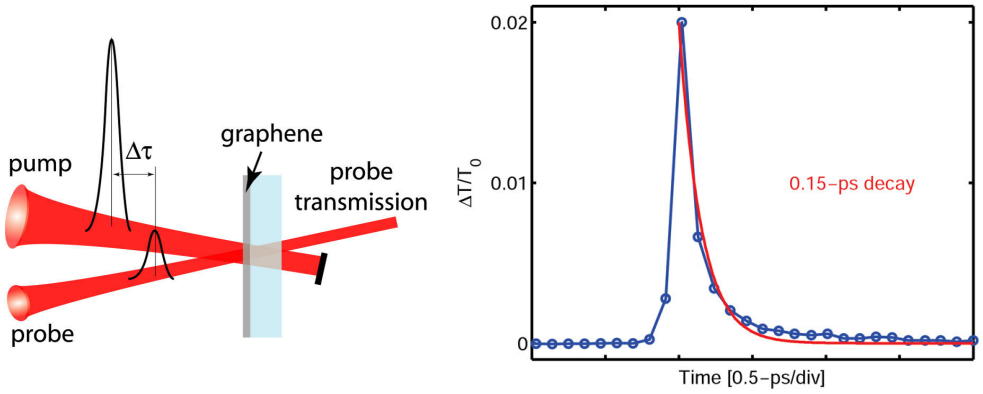

Figure 12: Optical pump-probe spectroscopy examines the multi-layer graphene sample's response to a 100-fs optical pulse and demonstrates saturable absorption with a transient (subpicosecond) 2% increase in transmission, above the steady state transmission (from [31]).

Theory predicts graphene's performance as a saturable absorber into the mid infrared, and experiments demonstrate its performance out to 2-μm wavelengths [20, 31]. This is useful since relatively few semiconductor saturable absorbers (SESAMs) have been created in the mid-infrared region (e.g. wavelengths beyond 2.2 μm). The semiconductor saturable absorber materials used in this region are GaAs [68], InGaAs [69], GaInSb/GaSb [70] and InAs/GaSb [71, 72, 73]. In addition, graphene has been reported to have larger modulation depths and lower saturation intensities than SESAMs [67].

Another beneficial attribute of graphene for use as a nonlinear optical material is its high optical damage threshold (near 100 GW/cm^2) [18] to allow saturable absorption without concern of damaging the graphene. In addition, graphene is a flexible thin film and can conformally coat materials. This enables bonding graphene devices to optics (e.g., mirrors) to produce integrated nonlinear optical devices, such as wavelength-independent saturable absorber mirrors (SAM). This is unlike conventional semiconductor SAMs which are engineered for specific wavelengths and are difficult to engineer at wavelengths longer than 2 μm (due to material issues). Thus, graphene may play a future role as a SAM for creating mode-locked lasers in the mid-IR region [31].

To investigate graphene's nonlinear susceptibility, third-harmonic generation (THG) experiments were performed. Graphene exhibited a strong THG when the excitation is in three-photon resonance with graphene at the M-point in its Brillouin zone [74]. At these high energies, graphene's bandstructure is no longer linear. A van Hove singularity at this point forms and creates a large joint density of states which leads to this significant optical response. The THG signal is over 100x larger than in glasses, and is polarization selective allowing determination of graphene's in-plane and out-of-plane nonlinear optical response [74]. Since the THG signal is in the UV spectral region this provides a unique method for identifying graphene monolayers. One such simple graphene identification system could use an 800-nm laser to excite the graphene and image the area with an optical filter that blocked 800-nm but passed the UV wavelengths. This system would have virtually no background scattered light since the excitation is in the visible or near infrared, and since there is relatively little stray UV light in the laboratory environment. This method of identifying graphene is similar to observations using multi-photon fluorescence microscopy, thereby allowing graphene's identification through modification of commercially available systems. In addition to identifying graphene monolayers, this THG technique provides insight into the physical dielectric properties of graphene.

Finally, another attraction to graphene as a nonlinear optical material is its reduced dimensionality, leading to reduced carrier density, as well as its linear density of states (DOS) as a function of energy. Applications including optical switches, gates and bi-stable devices may operate at lower power and over greater spectral bandwidths due to graphene's physical properties. Other potential fields for future graphene nonlinear optical devices include optical limiters and photothermal detectors.

3 Summary and Future Potential

The unique physical properties of graphene, and other 2D materials, enable a wealth of opportunities in photonics. Typically many electronic, photonic, and optical devices have been designed using bulk material properties which are often modified by surface effects. However, graphene is all surface with no bulk, and this (in part) is what makes the material so exciting. Its reduced-dimensionality and semi-metallic nature provide a linear energy-momentum dispersion with "massless" carriers and a zero bandgap Dirac point. These properties also enable graphene to exhibit fundamental physical effects like the fractional quantum Hall effect and universal optical conductance, which provides graphene with the interesting optical property of broadband linear absorption of 2.3% per monolayer.

Some of graphene's recent applications are in: electronics (FETs, touch screens, flexible electronics), optics (filters and saturable absorbers), photonics (photodetectors, polarizers, modulators), and plasmonics (sub-diffraction-limit photonics, polarization control and strong surface plasmon coupling in near IR for telecommunications). Graphene can be fabricated as large-area, mono- and multi-layer films. It can be processed into devices with conventional lithographic fabrication technology.

This report aimed to provide a basic understanding of the application of graphene in photonic devices, specifically for photodetection, optical modulation, optical polarization, plasmonics, and nonlinear optical devices. For these applications, graphene has notable properties that include high carrier mobility [16],

broad spectral absorption [17], high optical damage threshold [18], as well as low-irradiance nonlinear optical effects [74, 31].

Graphene is a candidate for carbon-based photonics [28] as well as photonic integrated circuits (PICs). This is primarily due to graphene's physical properties in three areas: electrical, mechanical, and optical. The photonic attributes in these three areas are summarized below.

Electrical: graphene furnishes electronic devices with its high carrier mobility and high conductivity (both thermal and electrical), and potential for ballistic carrier transport (carrier propagation like optical light in a waveguide).

Mechanical: graphene is strong yet flexible. Also, it can be transferred to conformally coat optics and other structures, thereby, imparting graphene's mechanical properties and creating hybrid materials.

Optical: the broad spectral nature of graphene is of particular interest. It operates as an optical absorber from the UV, through the visible, IR, and into the THz. Its operation in the THz region is also observed in THz transistors and plasmonic structures. At even lower frequencies it has potential for bolometers in the GHz and MHz, with particular emphasis on photon counting in these regions, which is of great interest for microwave quantum experiments and astronomy.

As previously noted, other reviews on this and similar subjects are available, and a few are listed here in such areas as: graphene photonics [3, 4, 5, 6], graphene electronics [7, 8], plasmonics [9], and 2D materials and heterostructures [10, 11]. These are a tiny subset of the large (and rapidly growing) field of graphene and two-dimensional materials. The near future seems to be directed towards molecular-scale modification of graphene's material properties (electronic, optic, plasmonic, photonic, etc.) through the use of heterostructures with other 2D materials as well as functionalization and intercalation of graphene.

Graphene has moved physics with the demonstration of a true two-dimensional material, which quantum well structures have approached but never fully achieved. The physics revealed by this reduction to two dimensions has created an explosion of interest, discovery, and application. New two-dimensional materials and quasi-2D structures are creating exciting opportunities in almost every field. Photonics gains a great deal from graphene's unique electrical, mechanical, and optical properties.

Acknowledgements

I appreciate helpful discussions, comments, and suggestions from Frank Bucholtz, Stan West, and Kurt Gaskill.

4 Glossary

Brillouin zone: The primitive cell formed in the reciprocal lattice of a periodic atomic structure. Any momentum can be mapped to a point in the Brillouin zone. By solving the energy-momentum dispersion relation (see below) the Brillouin zone representation shows the energy solutions for a given momentum.[75]

carrier mobility: The proportional relationship of the magnitude of drift velocity per applied electric field. Mobility is limited by carrier scattering from phonons (high-temperature) and/or lattice imperfections (low-temperatures).[76]

energy-momentum dispersion: Allowed solutions in a periodic crystalline solid which provide the energy band structure. Often Bloch functions are used as solutions to the Schrödinger equation to a simplified model of carrier(s) in a periodic potential.[75]

Dirac point: Certain materials have band structures which are best described by the Dirac equation rather than the more commonplace Schrödinger equation. The bandstructure in these systems often contains two conical surfaces in the Brillouin zones. These cones meet at their vertices, and this singularity is known as the Dirac point.

Fermi level: The term is often used synonymously with the chemical potential (even though these are equal only at T=0 K, at which point they are equal to the Fermi energy). At T=0, this is the highest filled energy state. The chemical potential is a function of temperature, and is a parameter in the Fermi-Dirac distribution function (which gives the occupation probability of an energy state in an ideal electron gas in thermal equilibrium).[76]

Franz-Keldysh effect: The modification of the band edge by the application of an electric field. This results in a change in the spectral absorption of the material.

Hall effect: The force on moving carriers in the presence of a magnetic field causes a transverse electric field to develop and verifies E.H. Hall's hypothesis (in 1879) that an increased resistance should be observed.

- **Quantum Hall effect:** The Hall effect in two-dimensional systems show a quantization of voltage as a magnetic field is continuously varied. The 1985 Nobel prize was awarded to Klaus von Klitzing for this discovery.
- **Fractional Quantum Hall effect:** The collective behavior of carriers in magnetic fields exhibit characteristics of particles with quantized fractional elementary charge. The 1998 Nobel prize was awarded to Robert Laughlin, Horst Störmer, and Daniel Tsui "for their discovery of a new form of quantum fluid with fractionally charged excitations."

Nonlinear susceptibility: Optical susceptibility relates an electric field in a material to the polarization (or dipole moment per unit volume), $\vec{P} = \chi\vec{E}$. In optics this is often expressed as a power series: $\vec{P} = \sum \chi^{(i)}\vec{E}^i$. The linear susceptibility term has $i = 1$, and the nonlinear susceptibility terms have $i > 1$, and are known as the second-, third-, ... i^{th} -order nonlinear optical susceptibilities.[77]

Pauli exclusion principle: Only one electron can occupy a single quantum state. To put this another way, no two electrons can have all their quantum numbers equal. [76]

Peltier effect: The cooling precipitated by an isentropic expansion of an ideal gas (e.g., free electron gas). For example, in semiconductors when a region of high-electron concentration is allowed to flow to a region of low-electron concentration, the electron gas expands and performs work to equalize the two chemical potentials, thereby resulting in Peltier cooling.[78]

Quantum-confined Stark effect: The energy levels created in a quantum confined system are modified by the application of an electric field. This occurs in the same manner as in atomic physics where the Stark effect demonstrates the shifting of energy levels in response to an applied electric field. This technique is often used to modify quantum-confined exciton states.[60]

Responsivity: A measure of the electrical output for a given optical input. The maximum responsivity varies with wavelength (λ) and with the conversion efficiency of photons to detected electrons (or quantum efficiency, η), and is described by the equation $R = \eta\lambda/1240$ [A/W], for λ in nanometers.

Surface plasmon polariton (SPP): The coupling of light with the 2D carriers can be described by surface plasmon polariton (SPP) (the term polariton derived from, "coupled electric ***polariz***ation-pho***ton*** waves").[60]

ultimate tensile strength: (also know as ultimate strength) The maximum stress which can be applied without breaking a material.

universal optical conductance: A macroscopic manifestation of quantum mechanics in which the optical (high-frequency) conductance of a material is expected to be frequency independent with a value $G(\omega) = G_0 \equiv \frac{\pi}{2} \cdot e^2/h$.[79]

van der Waals force: Force weaker than that of ionic and covalent bonds. Also know as the fluctuating dipole force. This weak bond is formed by the interaction of closely spaced dipoles which exhibit a net energy reduction. The force of this bond is weak and falls off rapidly with distance.[80]

van Hove singularity: A critical point occurs when the derivative of the energy with respect to momentum (dE/dk) is zero. At this point the density of states diverges producing a van Hove singularity. Instead of reaching infinity, the density of states are finite in a real system. This creates a large joint density of states and results in a large optical absorption at these singularity points.[60]

Young's modulus: (also known as elastic modulus) The stress divided by the strain acting in one dimension on an object.

References

[1] P. Wallace, "Band theory of graphite," Physical Review **71**, 622–634 (1947).

[2] K. S. Novoselov, A. K. Geim, S. V. Morozov, D. Jiang, Y. Zhang, S. V. Dubonos, I. V. Grigorieva, and A. A. Firsov, "Electric field in atomically thin carbon films," Science **306**, 666–669 (2004).

[3] P. Avouris and M. Freitag, "Graphene photonics, plasmonics, and optoelectronics," IEEE Journal on Selected Topics in Quantum Electronics **20** (2014).

[4] Q. Bao and K. P. Loh, "Graphene photonics, plasmonics, and broadband optoelectronic devices," ACS Nano **6**, 3677–3694 (2012).

[5] H. X. Wang, Q. Wang, K. G. Zhou, and H. L. Zhang, "Graphene in light: Design, synthesis and applications of photo-active graphene and graphene-like materials," Small **9**, 1266–1283 (2013).

[6] S. Yamashita, "A tutorial on nonlinear photonic applications of carbon nanotube and graphene," Journal of Lightwave Technology **30**, 427–447 (2012).

[7] J. S. Moon and D. K. Gaskill, "Graphene: Its fundamentals to future applications," IEEE Transactions on Microwave Theory and Techniques **59**, 2702–2708 (2011).

[8] D. M. Sun, C. Liu, W. C. Ren, and H. M. Cheng, "A review of carbon nanotube- and graphene-based flexible thin-film transistors," Small **9**, 1188–1205 (2013).

[9] A. N. Grigorenko, M. Polini, and K. S. Novoselov, "Graphene plasmonics," Nature Photonics **6**, 749–758 (2012).

[10] A. K. Geim and I. V. Grigorieva, "Van der waals heterostructures," Nature **499**, 419–425 (2013).

[11] Q. H. Wang, K. Kalantar-Zadeh, A. Kis, J. N. Coleman, and M. S. Strano, "Electronics and optoelectronics of two-dimensional transition metal dichalcogenides," Nature Nanotechnology **7**, 699–712 (2012).

[12] J.-H. Chen, C. Jang, S. Xiao, M. Ishigami, and M. S. Fuhrer, "Intrinsic and extrinsic performance limits of graphene devices on SiO_2," Nature Nanotechnology **3**, 206–209 (2008).

[13] S. Adachi, "GaAs, AlAs, and $Al_xGa_{1-x}As$: Material parameters for use in research and device applications," Journal of Applied Physics **58**, R1–R29 (1985).

[14] P. J. Burke, I. B. Spielman, J. P. Eisenstein, L. N. Pfeiffer, and K. W. West, "High frequency conductivity of the high-mobility two-dimensional electron gas," Applied Physics Letters **76**, 745–747 (2000).

[15] W. Pan, N. Masuhara, N. S. Sullivan, K. W. Baldwin, K. W. West, L. N. Pfeiffer, and D. C. Tsui, "Impact of disorder on the 5/2 fractional quantum hall state," Phys. Rev. Lett. **106**, 206806 (2011).

[16] Y. Zhang, Y. Tan, H. L. Stormer, and P. Kim, "Experimental observation of the quantum Hall effect and Berry's phase in graphene," Nature **438**, 201–204 (2005).

[17] R. R. Nair, P. Blake, A. N. Grigorenko, K. S. Novoselov, T. J. Booth, T. Stauber, N. M. R. Peres, and A. K. Geim, "Fine structure constant defines visual transparency of graphene," Science **320**, 1308 (2008).

[18] M. Currie, J. D. Caldwell, F. J. Bezares, J. Robinson, T. Anderson, H. Chun, and M. Tadjer, "Quantifying pulsed laser induced damage to graphene," Applied Physics Letters **99** (2011).

[19] J. Bonse, S. Baudach, J. Krger, W. Kautek, and M. Lenzner, "Femtosecond laser ablation of silicon-modification thresholds and morphology," Applied Physics A: Materials Science and Processing **74**, 19–25 (2002).

[20] G. Xing, H. Guo, X. Zhang, T. C. Sum, and C. H. A. Huan, "The physics of ultrafast saturable absorption in graphene," Optics Express **18**, 4564–4573 (2010).

[21] D. K. Gaskill and L. O. Nyakiti, "Formation of epitaxial graphene," in "Graphene Nanoelectronics," , R. Murali, ed. (Springer US, 2012), pp. 137–165.

[22] C. Berger, Z. Song, T. Li, X. Li, A. Y. Ogbazghi, R. Feng, Z. Dai, N. Alexei, M. E. H. Conrad, P. N. First, and W. A. De Heer, "Ultrathin epitaxial graphite: 2D electron gas properties and a route toward graphene-based nanoelectronics," Journal of Physical Chemistry B **108**, 19912–19916 (2004).

[23] B. L. VanMil, R. L. Myers-Ward, J. L. Tedesco, C. R. Eddy Jr., G. G. Jernigan, J. C. Culbertson, P. M. Campbell, J. M. McCrate, S. A. Kitt, and D. K. Gaskill, *Graphene formation on SiC substrates*, vol. 615 617 of *Materials Science Forum* (2009).

[24] S. Bae, H. Kim, Y. Lee, X. Xu, J.-S. Park, Y. Zheng, J. Balakrishnan, T. Lei, H. Ri Kim, Y. I. Song, Y.-J. Kim, K. S. Kim, B. Özyilmaz, J. H. Ahn, B. H. Hong, and S. Iijima, "Roll-to-roll production of 30-inch graphene films for transparent electrodes," Nature Nanotechnology **5**, 574–578 (2010).

[25] K. S. Kim, Y. Zhao, H. Jang, S. Y. Lee, J. M. Kim, K. S. Kim, J. . Ahn, P. Kim, J. . Choi, and B. H. Hong, "Large-scale pattern growth of graphene films for stretchable transparent electrodes," Nature **457**, 706–710 (2009).

[26] A. V. Eletskii, I. M. Iskandarova, A. A. Knizhnik, and D. N. Krasikov, "Graphene: fabrication methods and thermophysical properties," Physics-Uspekhi **54**, 227 (2011).

[27] J. D. Caldwell, T. J. Anderson, J. C. Culbertson, G. G. Jernigan, K. D. Hobart, F. J. Kub, M. J. Tadjer, J. L. Tedesco, J. K. Hite, M. A. Mastro, R. L. Myers-Ward, C. R. Eddy, P. M. Campbell, and D. K. Gaskill, "Technique for the dry transfer of epitaxial graphene onto arbitrary substrates," ACS Nano **4**, 1108–1114 (2010).

[28] J. T. Kim, Y.-J. Yu, H. Choi, and C.-G. Choi, "Graphene-based plasmonic photodetector for photonic integrated circuits," Opt. Express **22**, 803–808 (2014).

[29] C. Lee, X. Wei, J. W. Kysar, and J. Hone, "Measurement of the elastic properties and intrinsic strength of monolayer graphene," Science **321**, 385–388 (2008).

[30] M. Bernardi, M. Palummo, and J. C. Grossman, "Extraordinary sunlight absorption and one nanometer thick photovoltaics using two-dimensional monolayer materials," Nano Letters **13**, 3664–3670 (2013).

[31] M. Currie, T. Anderson, V. Wheeler, L. O. Nyakiti, N. Y. Garces, R. L. Myers-Ward, C. R. Eddy Jr., F. J. Kub, and D. K. Gaskill, "Mode-locked 2-μm wavelength fiber laser using a graphene-saturable absorber," Optical Engineering **52** (2013).

[32] W. S. Koh, C. H. Gan, W. K. Phua, Y. A. Akimov, and P. Bai, "The potential of graphene as an ITO replacement in organic solar cells: An optical perspective," IEEE Journal on Selected Topics in Quantum Electronics **20** (2014).

[33] H. Ito, S. Kodama, Y. Muramoto, T. Furuta, T. Nagatsuma, and T. Ishibashi, "High-speed and high-output InP-InGaAs unitraveling-carrier photodiodes," IEEE Journal on Selected Topics in Quantum Electronics **10**, 709–727 (2004).

[34] S. Gupta, M. Frankel, J. Valdmanis, J. Whitaker, G. Mourou, F. Smith, and A. Calawa, "Subpicosecond carrier lifetime in GaAs grown by molecular beam epitaxy at low temperatures," Applied Physics Letters **59**, 3276–3278 (1991).

[35] S. Chou, Y. Liu, W. Khalil, T. Hsiang, and S. Alexandrou, "Ultrafast nanoscale metal-semiconductor-metal photodetectors on bulk and low-temperature grown GaAs," Applied Physics Letters **61**, 819–821 (1992).

[36] M. Currie, F. Quaranta, A. Cola, E. M. Gallo, and B. Nabet, "Low-temperature grown GaAs heterojunction metal-semiconductor-metal photodetectors improve speed and efficiency," Applied Physics Letters **99** (2011).

[37] F. Xia, T. Mueller, Y. . Lin, A. Valdes-Garcia, and P. Avouris, "Ultrafast graphene photodetector," Nature Nanotechnology **4**, 839–843 (2009).

[38] T. Mueller, F. Xia, and P. Avouris, "Graphene photodetectors for high-speed optical communications," Nature Photonics **4**, 297–301 (2010).

[39] T. Mueller, F. Xia, M. Freitag, J. Tsang, and P. Avouris, "Role of contacts in graphene transistors: A scanning photocurrent study," Physical Review B - Condensed Matter and Materials Physics **79** (2009).

[40] M. Furchi, A. Urich, A. Pospischil, G. Lilley, K. Unterrainer, H. Detz, P. Klang, A. M. Andrews, W. Schrenk, G. Strasser, and T. Mueller, "Microcavity-integrated graphene photodetector," Nano Letters **12**, 2773–2777 (2012).

[41] A. Ferreira, N. M. R. Peres, R. M. Ribeiro, and T. Stauber, "Graphene-based photodetector with two cavities," Physical Review B - Condensed Matter and Materials Physics **85** (2012).

[42] X. Gan, R. Shiue, Y. Gao, I. Meric, T. F. Heinz, K. Shepard, J. Hone, S. Assefa, and D. Englund, "Chip-integrated ultrafast graphene photodetector with high responsivity," Nature Photonics **7** (2013).

[43] D. Sun, G. Aivazian, A. M. Jones, J. S. Ross, W. Yao, D. Cobden, and X. Xu, "Ultrafast hot-carrier-dominated photocurrent in graphene," Nature Nanotechnology **7**, 114–118 (2012).

[44] J. Yan, M. Kim, J. A. Elle, A. B. Sushkov, G. S. Jenkins, H. M. Milchberg, M. S. Fuhrer, and H. D. Drew, "Dual-gated bilayer graphene hot-electron bolometer," Nature Nanotechnology **7**, 472–478 (2012).

[45] K. C. Fong and K. C. Schwab, "Ultrasensitive and wide-bandwidth thermal measurements of graphene at low temperatures," Phys. Rev. X **3**, 031006 (2012).

[46] B. S. Karasik and A. V. Sergeev, "THz hot-electron photon counter," IEEE Trans. Appl. Supercond. **15**, 618 (2005).

[47] G. Konstantatos, M. Badioli, L. Gaudreau, J. Osmond, M. Bernechea, F. P. G. De Arquer, F. Gatti, and F. H. L. Koppens, "Hybrid graphene-quantum dot phototransistors with ultrahigh gain," Nature Nanotechnology **7**, 363–368 (2012).

[48] B. Y. Zhang, T. Liu, B. Meng, X. Li, G. Liang, X. Hu, and Q. J. Wang, "Broadband high photoresponse from pure monolayer graphene photodetector," Nature Communications **4** (2013).

[49] M. Liu, X. Yin, E. Ulin-Avila, B. Geng, T. Zentgraf, L. Ju, F. Wang, and X. Zhang, "A graphene-based broadband optical modulator," Nature **474**, 64–67 (2011).

[50] J. Yan, Y. Zhang, P. Kim, and A. Pinczuk, "Electric field effect tuning of electron-phonon coupling in graphene," Physical Review Letters **98** (2007).

[51] Y. Yu, Y. Zhao, S. Ryu, L. E. Brus, K. S. Kim, and P. Kim, "Tuning the graphene work function by electric field effect," Nano Letters **9**, 3430–3434 (2009).

[52] J. L. Bentez and D. Mendoza, "Modulation of the optical transmittance in multilayer graphene by an electrical signal," Applied Physics Letters **103** (2013).

[53] C. T. Ellis, A. V. Stier, M. H. Kim, J. G. Tischler, E. R. Glaser, R. L. Myers-Ward, J. L. Tedesco, C. R. Eddy, D. K. Gaskill, and J. Cerne, "Magneto-optical fingerprints of distinct graphene multilayers using the giant infrared kerr effect," Scientific Reports **3** (2013).

[54] Q. Bao, H. Zhang, B. Wang, Z. Ni, C. H. Y. X. Lim, Y. Wang, D. Y. Tang, and K. P. Loh, "Broadband graphene polarizer," Nature Photonics **5**, 411–415 (2011).

[55] Y. V. Bludov, M. I. Vasilevskiy, and N. M. R. Peres, "Tunable graphene-based polarizer," Journal of Applied Physics **112** (2012).

[56] J. A. Shackleford, R. Grote, M. Currie, J. E. Spanier, and B. Nabet, "Integrated plasmonic lens photodetector," Applied Physics Letters **94** (2009).

[57] N. Fang, H. Lee, C. Sun, and X. Zhang, "Sub-diffraction-limited optical imaging with a silver superlens," Science **308**, 534–537 (2005).

[58] A. Vakil and N. Engheta, "Transformation optics using graphene," Science **332**, 1291–1294 (2011).

[59] J. B. Khurgin and G. Sun, "Plasmonic enhancement of the third order nonlinear optical phenomena: Figures of merit," Optics Express **21**, 27460–27480 (2013).

[60] M. Fox, *Optical Propeties of Solids* (Oxford University Press, 2010), 2nd ed.

[61] Z. Q. Li, E. A. Henriksen, Z. Jiang, Z. Hao, M. C. Martin, P. Kim, H. L. Stormer, and D. N. Basov, "Dirac charge dynamics in graphene by infrared spectroscopy," Nature Physics **4**, 532–535 (2008).

[62] R. J. Koch, T. Seyller, and J. A. Schaefer, "Strong phonon-plasmon coupled modes in the graphene/silicon carbide heterosystem," Physical Review B - Condensed Matter and Materials Physics **82** (2010).

[63] S. Das Sarma and E. H. Hwang, "Collective modes of the massless Dirac plasma," Physical Review Letters **102** (2009).

[64] E. H. Hwang and S. Das Sarma, "Dielectric function, screening, and plasmons in two-dimensional graphene," Physical Review B - Condensed Matter and Materials Physics **75** (2007).

[65] F. H. L. Koppens, D. E. Chang, and F. J. Garca De Abajo, "Graphene plasmonics: A platform for strong light-matter interactions," Nano Letters **11**, 3370–3377 (2011).

[66] V. W. Brar, M. S. Jang, M. Sherrott, J. J. Lopez, and H. A. Atwater, "Highly confined tunable mid-infrared plasmonics in graphene nanoresonators," Nano Letters **13**, 2541–2547 (2013).

[67] Q. Bao, H. Zhang, Y. Wang, Z. Ni, Y. Yan, Z. X. Shen, K. P. Loh, and D. Y. Tang, "Atomic-layer graphene as a saturable absorber for ultrafast pulsed lasers," Advanced Functional Materials **19**, 3077–3083 (2009).

[68] J. Liu, Q. Wang, and P. Wang, "High average power picosecond pulse generation from a thulium-doped all-fiber MOPA system," Optics Express **20**, 22442–22447 (2012).

[69] R. C. Sharp, D. E. Spock, N. Pan, and J. Elliot, "190-fs passively mode-locked thulium fiber laser with a low threshold," Optics Letters **21**, 881–883 (1996).

[70] S. Kivist, T. Hakulinen, M. Guina, and O. G. Okhotnikov, "Tunable raman soliton source using mode-locked tm-ho fiber laser," IEEE Photonics Technology Letters **19**, 934–936 (2007).

[71] C. R. Pollock, N. A. Brilliant, D. Gwin, T. J. Carrig, W. J. Alford, J. B. Heroux, W. I. Wang, I. Vurgaftman, and J. R. Meyer, "Mode locked and Q-switched Cr:ZnSe laser using a semiconductor saturable absorbing mirror (SESAM)," in "OSA Trends in Optics and Photonics Series," , vol. 98 (2005), vol. 98, pp. 252–256.

[72] I. T. Sorokina, E. Sorokin, and T. J. Carrig, "Femtosecond pulse generation from a SESAM mode-locked Cr:ZnSe laser," in "Conference on Lasers and Electro-Optics and 2006 Quantum Electronics and Laser Science Conference, CLEO/QELS 2006," (2006).

[73] B. Bernhardt, E. Sorokin, P. Jacquet, R. Thon, T. Becker, I. T. Sorokina, N. Picqué, and T. W. Hänsch, "Mid-infrared dual-comb spectroscopy with 2.4 μm Cr 2+:ZnSe femtosecond lasers," Applied Physics B: Lasers and Optics **100**, 3–8 (2010).

[74] S. Y. Hong, J. I. Dadap, N. Petrone, P. C. Yeh, J. Hone, and R. M. Osgood Jr., "Optical third-harmonic generation in graphene," Physical Review X **3** (2013).

[75] S. Sze, *Physics of Semiconductor Devices* (Wiley, 1981).

[76] C. Kittel, *Introduction to Solid State Physics* (John Wiley & Sons, Inc., New York, 1986), 6th ed.

[77] R. Boyd, *Nonlinear Optics*, Nonlinear Optics (Academic Press, 2003).

[78] C. Kittel and H. Kroemer, *Thermal Physics* (W. H. Freeman, 1980).

[79] A. B. Kuzmenko, E. Van Heumen, F. Carbone, and D. Van Der Marel, "Universal optical conductance of graphite," Physical Review Letters **100** (2008).

[80] N. Ashcroft and N. Mermin, *Solid State Physics* (Saunders College, Philadelphia, 1976).